DOI: 10.1478/AAPP.1011A4

AAPP | Atti della Accademia Peloritana dei Pericolanti
Classe di Scienze Fisiche, Matematiche e Naturali
ISSN 1825-1242

Vol. 101, No. 1, A4 (2023)

MRI FARADAY CAGES: AN ALTERNATIVE PROTOCOL FOR SHIELDING EFFECTIVENESS MEASUREMENTS

GIUSEPPE ACRI [a], VALENTINA VENUTI [b], CARMELO ANFUSO [c], FRANCESCO CARIDI [b*], GIUSEPPE PALADINI [b], GIUSEPPE VERMIGLIO [d] AND DOMENICO MAJOLINO[b]

ABSTRACT. The periodic evaluation of the Faraday cage efficiency for diagnostic Magnetic Resonance is mandatory by Italian legislation and it is recommended by manufacturers. An inadequate shielding could affect clinical images with artifacts, reducing the quality of examinations. The International reference standard for shielding effectiveness measurements is represented by IEEE Standard 299-2006, but it results poorly applicable in Magnetic Resonance sites. In this study, an alternative approach is proposed to simplify the applicability of the IEEE Standard. The experimental set-up for measurements is composed by a signal generator and a transmitting antenna, coupled with the signal generator. The novelty of the proposed methodology consists in the absence of the receiver antenna; for this purpose, the Magnetic Resonance scanner is used. This approach permits to test the entire Faraday cage by means of a single measure. If the Magnetic Resonance device picks up the radiofrequency signal from outside of the cage, this would be visible on the acquired images as a "zipper" artifact. Four Faraday cages, different in building materials, were tested by using the proposed methodology, and the results were compared with those obtained by using the IEEE Standard. The presence of the "zipper" artifact on the images made us inspect the entire Faraday cage and not just the openings, finding that the radiofrequency signal entered from an area without openings, thus denoting a poor construction of the cage. The proposed methodology provides an immediate evaluation of the shielding efficiency, furnishing information on the entire Faraday cage and not only on its apertures. The method is simple, easily reproducible, and constitutes a valid alternative to the IEEE Standard; in particular, during constancy tests.

1. Introduction

Magnetic Resonance Imaging (MRI) is a highly sophisticated imaging modality, commonly used in clinical diagnosis (Capstick *et al.* 2008), which provides, in a non-invasive way, images of internal tissues without applying ionizing radiation (Lauterbur 1973; Mansfield 1977). MRI scanners combine three different magnetic fields, *i.e.*, the static magnetic field (typically symbolized by B_0), the radiofrequency (RF) field (B_1), and the magnetic field gradients in the three spatial directions ($\partial B/\partial x$, $\partial B/\partial y$ and $\partial B/\partial z$, respectively), that are switched on and off to select the region of interest for spatial encoding of image (Acri *et al.* 2018; Hartwig *et al.* 2009, 2022). The main goal of the MRI device is to produce

images that allow accurate and timely diagnoses (Torfeh *et al.* 2007). In order to guarantee the maintenance of a consistent image quality over the radiological equipment lifetime, it is necessary to establish and actively maintain regular and adequate quality-assurance (QA) procedures (Bonanno *et al.* 2019). As a matter of fact, MRI QA programs for images evaluation are well established (Acri *et al.* 2012; Firbank *et al.* 2000; Lerski and de Certaines 1993; Price *et al.* 1990). However, artifacts are a very common issue in MRI clinical use, they may be caused by the MR scanner hardware itself, by the interaction of the patient with the hardware, or generated by an external signal (Graves and Mitchell 2013). Artifacts may be confused with a pathology or can simply reduce the quality of examinations. The knowledge of the artifacts and their sources is extremely important in order to avoid false diagnoses and to learn how to eliminate them (Krupa and Bekiesińska-Figatowska 2015). In particular, one type of artifact may be due to the RF signal coming from outside of the Magnet room. It appears on the diagnostic image as a dashed line with a width of 1 or 2 pixels, called "zipper" (Zhuo and Gullapalli 2006), that extends in the frequency encoding direction, throughout the image series. It is important to highlight that MR scanner is a sensitive radio receiver, and if any outside radiofrequency gets into the MRI room, the scanner will pick it up. For this reason, all magnet rooms are shielded in order to eliminate interferences from devices, located outside the magnet room, that emit RF signals that could interfere with MR signal, and viceversa. This kind of shielding is called Faraday cage. These cages are usually realized using aluminum panels or copper sheets, and typically attenuation levels are from 70 to 130 dB. Attenuation levels below the aforementioned range could indicate a malfunctioning of the Faraday cage, with possible repercussions on the images. The efficacy of the Faraday cage is a parameter that must be verified both during acceptance test and during constancy measurements. In this context, Italian legislation (Ministero della Salute 2021) suggests periodic measurements of the efficacy of the Faraday cage at least annually. The IEEE 299-2006 - IEEE Standard Method for Measuring the Effectiveness of Electromagnetic Shielding Enclosures ("IEEE Standard Method for Measuring the Effectiveness of Electromagnetic Shielding Enclosures" 2007) represents the general reference for these measurements. In this reference the shielding efficacy is defined as follows: "*the ratio of the signal received (from a transmitter) without the shield, to the signal received inside the shield*". To evaluate shielding efficacy, the IEEE 299-2006 Standard measurements setup is composed of two calibrated antennas (transmitting and receiving), two shielded cables, a signal generation and a spectrum analyzer. The measurements must be conducted in the following ranges: a) low frequency range (LFR, 9 kHz – 20 MHz), b) resonance frequency range (RFR, 20 MHz – 300 MHz), c) high frequency range (HFR, 300 MHz – 18 GHz).

The physical quantities recommended by the IEEE 299-2006 Standard, to be measured as function of frequency, are reported in Table 1. For each measurement point, two different evaluations must be performed, the first one in absence of the shield and the second one with the interposition of the shield between the transmitting antenna and the receiving one. This kind of evaluation must be made using different antennas. The applicability of this standard to MRI Faraday cages appears quite complicated considering that, for each individual opening panel, measurements should be conducted for different positions. For this reason, practically, during acceptance and constancy controls, for each aperture of the Faraday cage only one measurement on a single position, for Electric field and Magnetic field respectively, is performed. Usually, the measurements on MRI Faraday cage are performed only on

TABLE 1. Physical quantities recommended by the IEEE 299-2006 Standard to be measured in the three frequency ranges: magnetic flux (H), or potential (V), in the low frequency range (LFR, 9 kHz – 20 MHz); electric field (E) in the resonant frequency range (RFR, 20 MHz – 300 MHz) and power (P) in the high frequency range (HFR, 300 MHz – 18 GHz).

	Frequency range		
	LFR 9 kHz – 20 MHz	RFR 20 MHz – 300 MHz	HFR 300 MHz – 18 GHz
Physical Quantities	H (or V)	E	P

critical points, which coincide with apertures of the Faraday cage: door of the Magnet room, view-window, filter panels, air-vent apertures and waveguides, and in none of these cases the IEEE 299-2006 Standard can be rigorously applied. In fact, air-vent apertures and waveguides are often excluded from measurements, due to the difficulty in the positioning of the measurement setup. Recently, a different approach was suggested in order to obtain door shielding measurement of MRI environment (Mirarchi *et al.* 2020). It is based on IEEE 299-2006 Standard procedures and needs some prerequisites, such as the removal of metallic equipment, and limitations as far as the number of people within the shielded enclosure is concerned. Following both the IEEE 299-2006 Standard and the methodology suggested in (Mirarchi *et al.* 2020), the shielding measurements can be performed only on MRI room apertures and no information can be deduced on the constructive accuracy of the entire Faraday cage. For example, it is not possible to check whether two panels have been badly welded.

In this study, we propose a different approach in measuring shielding efficacy, suitable during acceptance test, in conjunction with the IEEE 299-2006 standard, and constancy measurements, and consisting in a single measurement able to verify the effective shielding of the entire Faraday cage. The novelty is also present in the measurement setup, since only a signal generator and a biconic antenna, used as transmitter, are required. The receiver device is represented by the MRI scanner, thanks to its ability in producing diagnostic images without zipper artifacts. The new proposed procedure can provide an immediate determination of the shielding accuracy, guaranteeing the simplicity and reproducibility of the method as efficient tools for quick inspections.

2. Materials and methods

Before explaining the proposed method, it is worth remarking that the most common MRI total body scanners use field strengths of 0.35 T, 0.5 T, 1.5 T and 3 T. In the case of the hydrogen proton, the corresponding resonance frequencies are about 14.9 MHz, 21.3 MHz, 63.9 MHz and 127 MHz respectively. As established (Moser *et al.* 2009; Testagrossa *et al.* 2021), the MRI image is directly related to the resonance frequency of the MRI device. As a matter of fact, the center point of the field of view (FOV), defined by the size of two- or three-dimensional spatial encoding area of the MRI image, is the point where the magnetic field is B_0 and it corresponds to the resonance frequency of the device.

In Fig. 1 the representation of the FOV, in terms of position, magnetic gradients and frequencies is shown. The magnetic field at the center of the FOV, positioned in the center

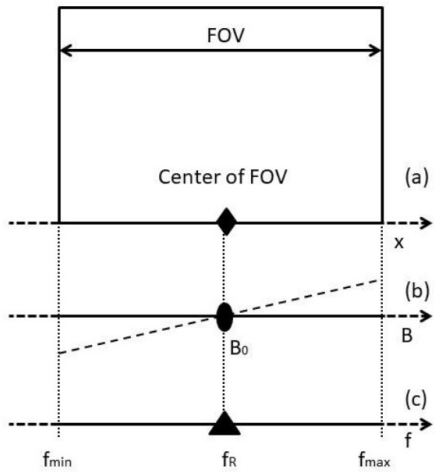

FIGURE 1. MRI FOV representation in terms of position, magnetic gradients and frequencies.

of the magnet bore (isocenter) is B_0 and the resonance frequency corresponds to:

$$f_r = \frac{\gamma}{2\pi} B_0 \tag{1}$$

where γ is the gyromagnetic ratio. Applying a linear magnetic field gradient along x-axis (G_x), that represents the variation of the magnetic field with respect to the x-coordinate, the field as function of position becomes:

$$B = B_0 \pm x G_x \tag{2}$$

and the frequency at any point along the axis is given by the following equation:

$$f_r = \frac{\gamma}{2\pi}(B_0 \pm x G_x). \tag{3}$$

Consequently,

$$f - f_r = \pm \frac{\gamma}{2\pi} x G_x. \tag{4}$$

This procedure represents the so-called frequency encoding, according to which the resonance frequency turns out to be proportional to the position of the selected slice. Practically, the entire FOV is around the Resonance Frequency.

Based on the aforementioned considerations, the experimental set-up used to test the shielding efficiency of the entire Faraday cage consists only in a signal generator (Hewelett

– Packard 8648C), working in the frequency range 100 kHz – 3200 MHz, output RF level ranging from –136 dBmW to + 20 dBmW, and a biconic transmitting antenna (VHBB 9124 – Schwarzbeck Mess Elektronik), working in the frequency range 30 – 300 MHz and having an isotropic gain of about 0 dBmW in 60 – 300 MHz range, connected by a cable. No receiver antenna is necessary to conduct measurements. The receiver consists, in fact, in the MRI device and its capability to acquire images. In order to perform measurements, the transmitting antenna is positioned far from the MRI room (Fig. 2) and, using the signal generator, a frequency around the Resonance Frequency of the MRI scanner is set. In this manner, the generated electromagnetic wave simulates an external RF signal, which invests the entire MRI Faraday cage. At the same time, the MRI scanner is acquiring a

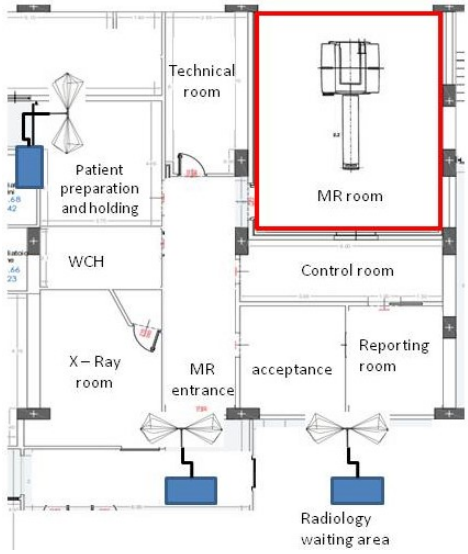

FIGURE 2. Examples of positioning of the experimental set-up, consisting in a signal generator and a biconic transmitting antenna. The transmitting antenna is positioned far from the magnet room, located in the upper right corner of the figure.

phantom image. If the generated radiofrequency wave gets inside the magnet room, it will be displayed on the acquired image as a dashed line along the spatial encoding, which represents the "zipper" artifact.

Faraday cage was also tested following the IEEE 299-2006 Standard. In this case, measurements were performed on the apertures of the cage, and carried out at four different frequencies.

3. Results

The proposed methodology was tested on four different MRI sites, namely MRI_1, MRI_2, MRI_3 and MR_4. In all sites, the magnetic field strength of the MRI devices was 1.5 T. The building materials of the Faraday cages were copper for MRI_1, aluminum

sheets for MRI_2 and MRI_3, copper and a large double glass with a copper grid inside it, positioned on the frontal surface, for MR_4, with the door of MRI room positioned on the same side. The power of the signal generator was set to +10 dBmW, while the distance between transmitting antenna and MRI Faraday cage for all the investigated sites is reported in Table 2.

TABLE 2. Investigated MRI sites, together with cage building materials of each site, distance between Faraday cage and transmitting antenna, obstacles encountered by the generated radiofrequency.

Site	Cage building materials	Distance (m)	Obstacles
MR_1	Copper	9.5	None
MR_2	Aluminum sheet	11.3	Perimetral walls
MR_3	Aluminum sheet	10.0	Walls
MR_4	Copper + (double glass with a metal grid inside on one side)	8.0	Walls

The MRI cages were tested using a frequency of 63.9 MHz. which is very close to the resonance frequency of the scanners. Two different motivations led us to consider this frequency: first of all, the measurement at the resonance frequency of the scanner is mandatory, and, in addition, if a "zipper" artifact occurs, it will certainly appear inside the FOV.

In Table 3 we show the results of the measurements conducted following the IEEE 299-2006 Standard and carried out at the resonance frequency of the MR scanner. In the same table, we also report the results obtained by applying the new methodology, always for a frequency of 63.9 MHz. As can be seen from an inspection of Table 3, in some points no measurements were performed using the IEEE 299-2006 Standard, because of the physical dimensions of the transmitting and receiving antennas.

TABLE 3. Shielding efficiency respectively evaluated using IEEE 299-2006 standard and by the proposed methodology.

Site	Frequency (MHz)	Aperture	Field	Antennas polarization (v: vertical, h:horizontal)	Attenuation (dBmW)	Proposed methodology
MRI_1	63.9	Door room View window Filter panel 1 Filter panel 2	E	h	98 96 Not applicable 94	No "zipper" artifact
MRI_2	63.9	Door room View window Filter panel 1 Filter panel 2	E	h	79 79 75 75	"Zipper" artifact on the acquired images
MRI_3	63.9	Door room View window Filter panel	E	h	87 82 80	Small dots that disappear when the signal generator power decreases
MRI_4	63.9	Door room View window Filter panel	E	h	81 81 Not applicable	Small dots that disappear when the signal generator power decreases

4. Discussion

By considering the results reported in Table 3, the evaluations conducted by applying the IEEE 299-2006 Standard highlighted acceptable values in all points, matching only with the cage openings. By applying the hereby proposed protocol, different scenarios were envisaged, which are discussed below.

- *MRI_1*: No "zipper" artifacts were visible on the acquired images. This result is consistent with the values obtained following the IEEE Standard.
- *MRI_2*: In this case, the measurements conducted following the IEEE Standard methodology highlighted acceptable shielding effectiveness values; however, on the acquired images the "zipper" artifact was visible (Fig. 3a). The power of the signal generator was gradually decreased, by steps of $+10$ dBmW, until it reached the value of -30 dBmW. Nevertheless, the "zipper" artifact was always visible on the acquired images, even if with lower intensity (Fig. 3b). By using a spectrum

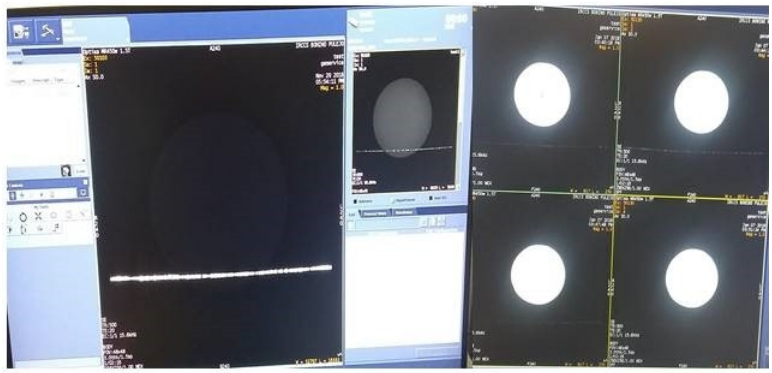

FIGURE 3. (a) Acquired image for MRI_2 at +10 dBmW; (b) Images sequence acquired at different power of the signal generator, with the "zipper" artifact visible in all images.

analyzer wired with a small loop antenna ("sniffing" loop), it was also possible to observe how the signal entered from a side wall, probably due to a gap between two panels, ascertaining a bad realization of the cage.
- *MRI_3*: The images acquired by MRI device highlighted small dots along the encoding frequency. By decreasing the signal generator power, the dots on the images disappeared, already by setting a power of -10 dBmW. It was possible to conclude that the Faraday cage has a good shielding efficiency, in agreement with the results obtained using the IEEE Standard.
- *MRI_4*: Also in this case small dots were visible on the acquired images. Setting a power of -10 dBmW on the signal generator, the zipper artifact disappeared, revealing a good shielding efficiency of the Faraday cage.

5. Conclusions

Even if, on one side, it is well-established that the methodology used by IEEE 299-2006 Standard represents the usual one in order to carry out efficiency measurements of Faraday cages, it has also to be pointed out, on the other side, that these standards are applied only on the cages apertures, considering that they were not drawn up specifically for MRI, but only adapted to it. In this context of little practicability of the standards, we propose a methodology able to test the entire Faraday cage by means of a single measure. The experimental set-up consists only in a signal generator coupled by a cable with a transmitting antenna, while the receiving antenna is represented by the MRI device during its regular operation of images acquisition. If the RF signal coming from outside of the Faraday cage is picked up by the MRI device, this would be visible on the acquired images as a "zipper" artifact, whose visualization testifies a bad attenuation of the Faraday cage.

The developed methodology provides an innovative, accurate, easily applicable and automated determination of the shielding efficiency of the entire MRI Faraday cage. It is an alternative to the commonly adopted procedures, which are typically complicated, and provides a real-time determination, confirming the flexibility of the method. These advantages, together with its simplicity and reproducibility, make this protocol an efficient tool for quick inspections.

References

Acri, G., Tripepi, M. G., Causa, F., Testagrossa, B., Novario, R., and Vermiglio, G. (2012). "Slice-thickness evaluation in CT and MRI: an alternative computerised procedure". *La radiologia medica* **117**(3), 507–518. DOI: 10.1007/s11547-011-0775-5.

Acri, G., Inferrera, P., Denaro, L., Sansotta, C., Ruello, E., Anfuso, C., Salmeri, F., Garreffa, G., Vermiglio, G., and Testagrossa, B. (2018). "dB/dt Evaluation in MRI Sites: Is ICNIRP Threshold Limit (for Workers) Exceeded?" *International Journal of Environmental Research and Public Health* **15**(7), 1298. DOI: 10.3390/ijerph15071298.

Bonanno, L., Marino, S., Morabito, R., Barbalace, G., Sestito, A., Testagrossa, B., and Acri, G. (2019). "Evaluation of US and MRI techniques for carotid stenosis: a novel phantom approach". *La radiologia medica* **124**(5), 368–374. DOI: 10.1007/s11547-018-0971-7.

Capstick, M., McRobbie, D., Hand, J., Christ, A., Kühn, S., Mild, K. H., Cabot, E., Li, Y., Melzer, A., Papadak, A., Prüssmann, K., Quest, R., Rea, M., Ryf, S., Oberle, M., and Kuster, N. (2008). *An investigation into occupational exposure to electromagnetic fields for personnel working with and around medical magnetic resonance imaging equipment*. Tech. rep. VT/2007/017. European Commission. Employment, Social Affairs and Equal Opportunities DG. URL: https://itis.swiss/assets/Downloads/Papers-Reports/Reports/VT2007017FinalReportv04.pdf (visited on 02/18/2023).

Firbank, M. J., Harrison, R. M., Williams, E. D., and Coulthard, A. (2000). "Quality assurance for MRI: practical experience." *The British Journal of Radiology* **73**(868), 376–383. DOI: 10.1259/bjr.73.868.10844863.

Graves, M. J. and Mitchell, D. G. (2013). "Body MRI artifacts in clinical practice: A physicist's and radiologist's perspective". *Journal of Magnetic Resonance Imaging* **38**(2), 269–287. DOI: 10.1002/jmri.24288.

Hartwig, V., Giovannetti, G., Vanello, N., Lombardi, M., Landini, L., and Simi, S. (2009). "Biological Effects and Safety in Magnetic Resonance Imaging: A Review". *International Journal of Environmental Research and Public Health* **6**(6), 1778–1798. DOI: 10.3390/ijerph6061778.

Hartwig, V., Sansotta, C., Morelli, M. S., Testagrossa, B., and Acri, G. (2022). "Occupational Exposure Assessment of the Static Magnetic Field Generated by Nuclear Magnetic Resonance Spectroscopy: A Case Study". *International Journal of Environmental Research and Public Health* **19**(13), 7674. DOI: 10.3390/ijerph19137674.

"IEEE Standard Method for Measuring the Effectiveness of Electromagnetic Shielding Enclosures" (2007). *IEEE Std 299-2006 (Revision of IEEE Std 299-1997)*, 1–52. DOI: 10.1109/IEEESTD.2007.323387.

Krupa, K. and Bekiesińska-Figatowska, M. (2015). "Artifacts in Magnetic Resonance Imaging". *Polish Journal of Radiology* **80**, 93–106. URL: https://www.ncbi.nlm.nih.gov/pmc/articles/PMC4340093/.

Lauterbur, P. C. (1973). "Image Formation by Induced Local Interactions: Examples Employing Nuclear Magnetic Resonance". *Nature* **242**(5394), 190–191. DOI: 10.1038/242190a0.

Lerski, R. A. and de Certaines, J. D. (1993). "Performance assessment and quality control in MRI by Eurospin test objects and protocols". *Magnetic Resonance Imaging* **11**(6), 817–833. DOI: 10.1016/0730-725X(93)90199-N.

Mansfield, P. (1977). "Multi-planar image formation using NMR spin echoes". *Journal of Physics C: Solid State Physics* **10**(3), L55–L58. DOI: 10.1088/0022-3719/10/3/004.

Ministero della Salute (2021). "Decreto 14 Gennaio 2021". *Gazzetta Ufficiale della Repubblica Italiana*. GU Serie Generale n.65 del 16-03-2021, 21A01353. URL: https://www.gazzettaufficiale.it/eli/id/2021/03/16/21A01353/sg.

Mirarchi, L., Giaquinto, V., Silvestri, S., and Massa, R. (2020). "A Standard Protocol Proposal for Reliable and Time-Saving Shielding Effectiveness Measurements for MRI Faraday Cages". *The Open Biomedical Engineering Journal* **14**(1), 1–10. DOI: 10.2174/1874120702014010001.

Moser, E., Stadlbauer, A., Windischberger, C., Quick, H. H., and Ladd, M. E. (2009). "Magnetic resonance imaging methodology". *European Journal of Nuclear Medicine and Molecular Imaging* **36**(S1), 30–41. DOI: 10.1007/s00259-008-0938-3.

Price, R. R., Axel, L., Morgan, T., Newman, R., Perman, W., Schneiders, N., Selikson, M., Wood, M., and Thomas, S. R. (1990). "Quality assurance methods and phantoms for magnetic resonance imaging: Report of AAPM nuclear magnetic resonance Task Group No. 1". *Medical Physics* **17**(2), 287–295. DOI: 10.1118/1.596566.

Testagrossa, B., Ruello, E., Gurgone, S., Denaro, L., Sansotta, C., Salmeri, F. M., and Acri, G. (2021). "Radio Frequency MRI coils and safety: how infrared thermography can support quality assurance". *Egyptian Journal of Radiology and Nuclear Medicine* **52**, 1–8. DOI: 10.1186/s43055-021-00659-y.

Torfeh, T., Beaumont, S., Guédon, J.-P., Normand, N., and Denis, E. (2007). "Software tools dedicated for an automatic analysis of the CT scanner quality control images". In: *Medical Imaging 2007: Physics of Medical Imaging*. Ed. by J. Hsieh and M. J. Flynn. Vol. 6510. SPIE, 65104G. DOI: 10.1117/12.707343.

Zhuo, J. and Gullapalli, R. P. (2006). "MR Artifacts, Safety, and Quality Control". *RadioGraphics* **26**(1), 275–297. DOI: 10.1148/rg.261055134.

[a] Università degli Studi di Messina,
Dipartimento di Scienze Biomediche, Odontoiatriche, e delle Immagini Morfologiche e Funzionali,
c/o A.O.U. Policlinico "G. Martino", Via Consolare Valeria 1, 98125 Messina, Italy

[b] Università degli Studi di Messina,
Dipartimento di Scienze Matematiche e Informatiche, Scienze Fisiche e Scienze della Terra,
Viale Ferdinando Stagno d'Alcontres 31, 98166 Messina, Italy

[c] IRCCS Centro Neurolesi "Bonino-Pulejo",
Strada Statale 113, C.da Casazza, 98124 Messina, Italy

[d] Medical physicist (freelance),
Via Regina Elena, Faro Superiore, 98158 Messina, Italy

[*] To whom correspondence should be addressed | email: fcaridi@unime.it

Communicated 24 May 2022; manuscript received 8 July 2022; published online 26 February 2023